Thin Fisher zeros

B P Dolan[1,2], W Janke[3], D A Johnston[4] and M Stathakopoulos[4]

[1] Department of Mathematical Physics, National University of Ireland, Maynooth, Republic of Ireland
[2] School of Theoretical Physics, Dublin Institute for Advanced Studies, 10, Burlington Road, Dublin, Republic of Ireland
[3] Institut für Theoretische Physik, Universität Leipzig, Augustusplatz 10/11, D-04109 Leipzig, Germany
[4] Department of Mathematics, Heriot-Watt University, Riccarton, Edinburgh EH14 4AS, UK

Abstract
Various authors have suggested that the loci of partition function zeros can profitably be regarded as phase boundaries in the complex temperature or field planes. We obtain the Fisher zeros for Ising and Potts models on non-planar ('thin') regular random graphs using this approach, and note that the locus of Fisher zeros on a Bethe lattice is identical to the corresponding random graph. Since the number of states q appears as a parameter in the Potts solution the limiting locus of chromatic zeros is also accessible.

PACS numbers: 05.50.+q, 05.45.-a

1. Introduction

The idea that studying the zeros of the partition function of a statistical mechanical model when a physical parameter was extended to complex values might provide valuable insights on critical behaviour in lattice models was first promulgated by Lee and Yang [1] for field-driven transitions and later by Fisher and others for temperature-driven transitions [2, 3]. Recently the study of such zeroes has also been extended to non-equilibrium situations such as directed percolation, with interesting results [4]. Although there has been a considerable body of work studying the partition function zeros of the Ising and Potts models on various regular lattices, most notably in recent years in [5, 6], there has been little investigation of the spin models on lattices exhibiting some form of geometrical disorder, such as random graphs, both for the annealed and quenched case. Some cases that have been investigated such as Penrose tilings have revealed intricate structure for the Fisher (complex temperature) zeros away from the real axes, while still possessing Onsager scaling behaviour at the physical critical point [7]. Others, such as the Ising model on annealed ensembles of planar ϕ^4 random graphs and the dual quad-rangulations, possess Fisher zeros which do lie on curves in the complex temperature plane [8], but which are different from the double-circle locus of the regular square lattice. This in itself

is interesting, since it shows that a distinct locus still exists when a sum over a class of graphs is folded into the partition function along with a sum over spin configurations. For both planar[5] and generic, non-planar random graphs perturbative calculations strongly suggest that the Lee–Yang (complex field) zeros still lie on the unit circle in the complex activity plane [8, 9], even though the technical assumptions of the original Lee–Yang theorem no longer apply in this case.

The previous work on both fat and thin random graph models has relied entirely on perturbative expansions and Monte Carlo simulations to investigate the various loci of zeros. There is rather more information at hand in both these cases, however, since exact evaluations of the partition function are possible in the thermodynamic limit using matrix integral/orthogonal polynomial methods in the planar case and a straightforward saddle-point calculation in the non-planar case. In the case of the Ising model on regular two-dimensional lattices the particular form of the solution for the free energy, as a double trigonometrical integral over a logarithm, allowed a direct identification of the loci of zeros as the curves or regions where the argument of the logarithm was zero. The fat and thin random graph solutions no longer have this form—they are even simpler, being directly the logarithms of algebraic expressions, which differ in the high- and low-temperature phases but match at the transition point, as they should.

The general question of how to extract loci of zeros for models with first-order transitions when one has some analytical expression or approximation for the partition function or free energy available has recently been addressed by Biskup *et al* [10]. They showed that under suitable technical conditions the partition function of a d-dimensional statistical mechanical model defined in a periodic volume $V = L^d$ which depends on a complex parameter z can be written in terms of complex functions $f_l(z)$ describing k different phases as

$$Z = \sum_l^k q_l e^{-\beta f_l V} + O(e^{-L/L_0} e^{-\beta f V}) \tag{1}$$

where q_l is the degeneracy of phase l, β is the inverse temperature and L_0 is of the order of the correlation length. The various f_l are to be interpreted as the metastable free energies of the phases, with $\mathrm{Re}\, f_l = f$ characterizing the free energy when phase l is stable. The zeros of the partition function are then determined to lie within $O(e^{-L/L_0})$ of the solutions of the remarkably simple equations

$$\mathrm{Re}\, f_{l,L}^{\mathrm{eff}} = \mathrm{Re}\, f_{m,L}^{\mathrm{eff}} < \mathrm{Re}\, f_{k,L}^{\mathrm{eff}} \qquad \forall k \neq l, m$$
$$\beta V (\mathrm{Im}\, f_{l,L} - \mathrm{Im}\, f_{m,L}) = \pi \bmod 2\pi \tag{2}$$

where $f_l^{\mathrm{eff}} = f_l - (\beta V)^{-1} \log q_l$. Since we have written an expression for Z that incorporates phase co-existence we are implicitly looking at models with first-order transitions, the canonical example being the field-driven transition for the Ising model.

The equations (2) show that zeros of Z asymptotically lie on the complex phase coexistence curves $\mathrm{Re}\, f_{l,L} = \mathrm{Re}\, f_{m,L}$ in the complex z-plane. Indeed, the idea that the loci of zeros might be thought of as Stokes lines which separate different asymptotic behaviours and that the real part of the free energy in the various phases should match along the lines is already implicit in [3, 5].

It might appear erroneous to attempt to apply the results of [10], formulated for first-order transitions and based on ideas arising from phase co-existence, to models where the physical temperature-driven transition is continuous. However, when considered in the complex

---

[5] We denote the planar graphs as 'fat' graphs since they can be thought of as being generated by the Feynman diagrams in a matrix theory which has fat, or ribbon-like, propagators that carry one matrix index on each side. The fatness of the propagators allows the identification of a surface with a given graph and helps in enforcing planarity. The converse is that generic random graphs appear as the Feynman diagrams in a theory with 'thin' propagators that carry no edge labels and which have no surface interpretation.

temperature plane such transitions will be continuous only at the physical point itself and possibly some other finite set of points. This can be seen by looking at expressions for the magnetization for the Ising model, for example, on the square lattice, on fat ϕ^4 graphs and on thin ϕ^3 graphs:

$$M = \frac{(1+u)^{1/4}(1-6u+u^2)^{1/8}}{(1-u)^{1/2}} \qquad \text{(square)}$$

$$M = \frac{3(1-16c^2)^{1/2}}{3-8c^2} \qquad \text{(fat } \phi^4) \qquad (3)$$

$$M = \frac{(1-3c)^{1/2}}{(1-2c)(1+c)^{1/2}} \qquad \text{(thin } \phi^3)$$

where $u = c^2 = \exp(-4\beta)$. The expressions for M apply through the complex extension of the low-temperature phase, and M will be zero outside this region. We can thus see that although M will vanish continuously at the physical critical points, $u = 3 - 2\sqrt{2}$, $c = 1/4$, $c = 1/3$ respectively, it will generically be non-zero at the phase boundary approaching from within the low-temperature region, whereas it will be zero approaching from outside. There are further discrete points where the magnetization vanishes continuously: at the anti-ferromagnetic point $u = 3 + 2\sqrt{2}$ and the unphysical point $u = -1$ on the square lattice; and the unphysical point $c = -1/4$ on the planar ϕ^4 graphs. It should also be remarked that the apparent singularities in the expressions for M at[6] $u = 1$, $c = \sqrt{3/8}$ and $c = 1/2$ respectively are spurious since they lie outside the domain of applicability of the expressions. Since we only have a discrete set of points along the phase boundary where M vanishes continuously, a typical point will be first order in nature and the arguments of [10] may safely be deployed to determine the locus of zeros.

The results of [3, 5, 10] give a very natural interpretation of the loci of partition function zeros as phase coexistence curves for suitably complex extended phases, both for Lee–Yang and Fisher zeros. Such a picture is also in accordance with the 'dynamical systems' determination of partition function zeros [11] for models which may be defined in terms of some sort of recursive renormalization group map. In these cases the loci of zeros appear as the Julia set of the map—in other words, the boundaries of the basins of attraction for the map, or phase boundaries of the complex extended phases.

In this paper we find the locus of Fisher zeros for the Ising model on three- and four-regular non-planar random graphs [12, 13], where such an expression can be calculated by saddle point methods and on the corresponding Bethe lattices where rather different recursive methods arrive at an identical answer. As a warm-up exercise we show that the methods employed in the study of three- and four-regular graphs also reproduce the known results for zeros that have been obtained by transfer matrix methods [14] in the one-dimensional[7] Ising model. The q-state Potts model on three- and four-regular random lattices may be treated in a similar manner to the Ising model and the locus of Fisher zeros obtained for general q. Since q appears in the solution for the q-state Potts model as a parameter we are also at liberty to look at chromatic zeros for our random graphs, which involves looking at the saddle point solutions for the ground state of the anti-ferromagnetic Potts model in the complex q-plane.

---

[6] $c = -1$ marks the start of a cut on the negative real axis.
[7] That is, on a two-regular graph.

2. Ising model in one dimension

The partition function for the Ising model with Hamiltonian

$$-\beta H = \beta \sum_{\langle ij \rangle} \sigma_i \sigma_j \qquad (4)$$

where $\sigma_i = \pm 1$, on two-regular random graphs with n vertices (i.e. on a one-dimensional ring) may be written as [12, 13]

$$Z_n(\beta) \times N_n = \frac{1}{2\pi i} \oint \frac{dg}{g^{n+1}} \int \frac{d\phi_+ \, d\phi_-}{2\pi \sqrt{\det K}} \exp(-S) \qquad (5)$$

where N_n is the number of undecorated rings and K is defined by

$$K_{ab}^{-1} = \begin{pmatrix} 1 & -c \\ -c & 1 \end{pmatrix}. \qquad (6)$$

The action itself is a direct transcription of the matrix model action [15] to scalar variables

$$S = \frac{1}{2} \sum_{a,b} \phi_a K_{ab}^{-1} \phi_b - \frac{g}{2} \left(z\phi_+^2 + \frac{1}{z}\phi_-^2 \right) \qquad (7)$$

with $z = \exp(h)$ and $c = \exp(-2\beta)$. In the above ϕ_+^2 can be thought of as representing 'up' spin vertices and ϕ_-^2 'down' spin vertices. Since the integral is Gaussian we are not obliged to pursue the saddle-point evaluation that is necessary in the next section for three- and four-regular graphs—we can simply carry out the integral directly. Scaling away the vertex counting factor of g we find that the free energy per site is given by the logarithm of the dominant eigenvalue of the quadratic form in the propagator,

$$
\begin{aligned}
f &\sim \log(\lambda_\pm) \\
\lambda_\pm &= \frac{-(1-z)^2 \pm \sqrt{(1-z^2)^2 + 4c^2 z^2}}{2z}.
\end{aligned}
\qquad (8)
$$

The partition function zeros and hence free energy singularities appear when the square root in the above expression is zero and both roots can contribute

$$(1-z^2)^2 + 4c^2 z^2 = 0 \qquad (9)$$

which recovers the equation for the Lee–Yang edge derived in [14].

3. Ising model on thin random graphs

The partition function for the Ising model with the Hamiltonian of equation (4) on three-regular random graphs with $2n$ vertices may be written as [12, 13]

$$Z_n(\beta) \times N_n = \frac{1}{2\pi i} \oint \frac{dg}{g^{2n+1}} \int \frac{d\phi_+ \, d\phi_-}{2\pi \sqrt{\det K}} \exp(-S) \qquad (10)$$

where N_n is now the number of undecorated (no-spin) ϕ^3 graphs. K is defined as above and the action now has the appropriate potential for generating ϕ^3 graphs

$$S = \frac{1}{2} \sum_{a,b} \phi_a K_{ab}^{-1} \phi_b - \frac{g}{3}(\phi_+^3 + \phi_-^3). \qquad (11)$$

It is necessary to include the counting factor N_n to disentangle the factorial growth of the undecorated graphs from any non-analyticity due to phase transitions in the decorating spins. One is also obliged to pick out the $2n$th order in the expansion explicitly with the contour

integral over g as, unlike the planar graphs of two-dimensional gravity, g cannot be tuned to a critical value to cause a divergence.

The mean-field Ising transition manifests itself in this formalism as an exchange of dominant saddle points. Solving the saddle point equations $\partial S/\partial \phi_\pm = 0$

$$\phi_+ = \phi_+^2 + c\phi_- \tag{12}$$
$$\phi_- = \phi_-^2 + c\phi_+$$

which we have rescaled to remove g and an irrelevant overall factor, we find a symmetric high-temperature solution

$$\phi_+ = \phi_- = 1 - c \tag{13}$$

which bifurcates at $c = 1/3$ to the low-temperature solutions

$$\phi_+ = \frac{1 + c + \sqrt{1 - 2c - 3c^2}}{2} \tag{14}$$
$$\phi_- = \frac{1 + c - \sqrt{1 - 2c - 3c^2}}{2}.$$

The bifurcation point is determined by the value of c at which the high- and low-temperature solutions for ϕ are identical, which appears at the zero of the Hessian $\det(\partial^2 S/\partial \phi^2)$. The magnetization order parameter for the Ising model can also be transcribed directly from the matrix model [15]

$$M = \frac{\phi_+^3 - \phi_-^3}{\phi_+^3 + \phi_-^3} \tag{15}$$

and shows a continuous transition with mean-field critical exponent ($\beta = 1/2$). The other critical exponents may also be calculated and take on mean-field values.

If one carries out a saddle point evaluation of equation (10), the leading term in the free energy will be given by an expression of the form $f \sim \log S$, where S is the action (11) evaluated at either the low- or high-temperature saddle point solutions for ϕ in equations (13), (14). Since we wish to match Re f between phases in order to find the loci of the partition function zeros we are demanding in this case

$$|S_L| = |S_H| \tag{16}$$

where S_L is the low-temperature saddle-point solution and S_H is the high-temperature saddle-point solution, both to be taken for complex c

$$S_H = \tfrac{1}{3}(1 - c)^3 \tag{17}$$
$$S_L = \tfrac{1}{6}(1 + c)^2(1 - 2c).$$

The resulting locus of Fisher zeros is shown in figure 1, and is slightly unusual in that it is not a closed curve as is usually the case for Ising and Potts models on regular lattices, but rather a cusp. It is not unique in not being a closed curve, however, since the the locus of the Fisher zeros for the one-dimensional Ising model is all of the imaginary axis[8]. For one-dimensional Potts models a similar result holds, with the zeros lying on a vertical line in the $\exp(-2\beta)$ plane passing through the real axis at $1 - q/2$. The random graph Ising model has mean-field exponents because of the locally treelike structure, so the scaling relation relating the angle ψ which the zeros make as they approach the real axis, the critical heat exponent α and the two critical amplitudes A_+, A_-,

$$\tan[(2 - \alpha)\psi] = \frac{\cos(\pi\alpha) - A_+/A_-}{\sin(\pi\alpha)} \tag{18}$$

---

[8] The one-dimensional locus of Fisher zeros can be found by applying the field/temperature duality unique to the one-dimensional case to the Lee–Yang zeros on the unit circle.
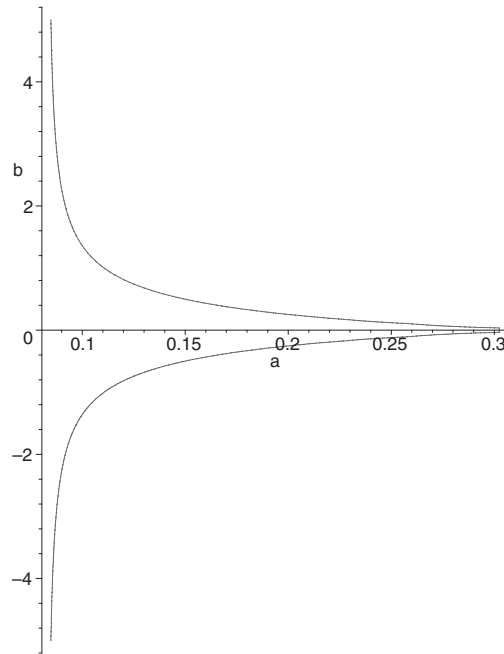
Figure 1. The locus of Fisher zeros in the complex $c = \exp(-2\beta)$ plane for the Ising model on ϕ^3 random graphs. The real and imaginary parts of c are denoted by a and b respectively. The cut on the negative real axis is not shown.

predicts[9] $\psi = \pi/4$. This is indeed what is observed at the cusp of the locus ($c = 1/3$) in figure 1. There is also a cut running along the negative real c axis from $c = -1$ to $c = -\infty$. At the start of the cut at $c = -1$ there is singular behaviour with the non-mean-field exponents $\alpha = 2$, $\beta = -1/2$ (a divergent magnetization) and $\gamma = 1$.

It should be remarked that a little care is needed in applying equation (16) since the presence of the modulus signs means that one runs of risk of picking up 'wrong sign' solutions. This is easily resolved when the complex phases are extensions of real phases as in the present case, when the behaviour on the real axis can be examined to make sure that the correct sign has been chosen.

The determination of the Fisher zero locus on other random regular graphs proceeds in the same manner as on the ϕ^3 graphs. On ϕ^4 (four-regular) graphs, for instance the action becomes

$$S = \frac{1}{2} \sum_{a,b} \phi_a K_{ab}^{-1} \phi_b - \frac{g}{4}(\phi_+^4 + \phi_-^4) \tag{19}$$

and the saddle-point solutions are

$$\phi_+ = \phi_- = \sqrt{1 - c} \tag{20}$$

---

[9] $\alpha = 0$, $A_+/A_- = 0$. Note that the original discussion was in terms of $u = c^2$, but since we are dealing with conformal transformations any conclusions about angles will still hold, as can easily be confirmed by plotting the locus directly in terms of u.

and

$$\phi_+ = \frac{1}{4c}\left(\sqrt{2 + 2\sqrt{1 - 4c^2}}\right)\left(1 - \sqrt{1 - 4c^2}\right)$$
$$\phi_- = \tfrac{1}{2}\left(\sqrt{2 + 2\sqrt{1 - 4c^2}}\right) \tag{21}$$

at high and low temperatures, respectively. These lead to the saddle-point actions

$$S_H = -c + \tfrac{1}{2} + \tfrac{1}{2}c^2$$
$$S_L = \tfrac{1}{4} - \tfrac{1}{2}c^2 \tag{22}$$

which are matched in the same manner as for the ϕ^3 graphs and also lead to a cusp locus, with the cusp now at $c = 1/2$.

Both the ϕ^3 and ϕ^4 curves appear rather like a folium of Descartes with the loop that would lie to the right of the cusp excised. The ϕ^3 curve turns out to have a rather more complicated formula

$$\frac{27}{16}y^2 = \frac{-(1 + \tfrac{9}{2}x + \tfrac{27}{16}x^2 + \tfrac{27}{4}x^3) + (1 + 3x)^{3/2}}{(1 + 4x)} \tag{23}$$

which is deduced from expressing $|S_H| = |S_L|$ in terms of the real, $x = \mathrm{Re}\, v$, and imaginary, $y = \mathrm{Im}\, v$, parts of $v = c - 1/3$. However, the expression for the ϕ^4 curve

$$y^2 = \frac{-x^2(x - \tfrac{1}{4})}{(x + \tfrac{1}{4})} \tag{24}$$

where $x = \mathrm{Re}\, v$, $y = \mathrm{Im}\, v$ and $v = c - 1/2$ is indeed a rescaling of the standard folium. There is also another branch of the locus of zeroes which is a reflection of this in the $\mathrm{Im}\, c$ axis.

4. Ising model on Bethe lattice

We now turn to the Ising model on a Bethe lattice, with co-ordination number m. The free energy per site is arrived at in an apparently very different manner to the random graphs by considering a recursion relation on the branches of the tree and is given by

$$\beta f = -\tfrac{1}{2}m\beta - \tfrac{1}{2}m\ln(1 - c^2) + \tfrac{1}{2}\ln[c^2 + 1 - c(x + x^{-1})] + \tfrac{1}{2}(m - 2)\ln(x + x^{-1} - 2c) \tag{25}$$

where c is again equal to $\exp(-2\beta)$ and x, defined implicitly by

$$x = \frac{e^{-2\beta} + e^{-2h}x^{m-1}}{1 + e^{-2h-2\beta}x^{m-1}} \tag{26}$$

emerges as the fixed point of the recursion. This model has a phase transition at $\beta_c = \tfrac{1}{2}\ln[m/(m - 2)]$ and the magnetization per site is

$$M = \frac{e^{2h} - x^m}{e^{2h} + x^m} \tag{27}$$

which ranges from -1 for $x \to \infty$ to $+1$ for $x = 0$. The derivation of these equations can be found in [16].

If we restrict ourselves to $h = 0$ and $m = 3$ in order to compare with the Fisher zeros on ϕ^3 graphs, the solutions of equation (26) are given by

$$x = 1$$
$$x = \frac{1 - c \pm \sqrt{1 - 2c - 3c^2}}{2c} \tag{28}$$

with $x = 1$ being a high-temperature solution (since $M = 0$ in this case) and the others being low-temperature solutions when $T < T_c$. If we substitute these into equation (25) we find

$$\beta f_{\mathrm{H}} = -\tfrac{3}{2}\beta - \tfrac{3}{2}\log(1 - c^2) + \tfrac{1}{2}\log[2(1 - c)^3]$$
$$\beta f_{\mathrm{L}} = -\tfrac{3}{2}\beta - \tfrac{3}{2}\log(1 - c^2) + \tfrac{1}{2}\log[(1 + c)^2(1 - 2c)] \tag{29}$$

where we have deliberately kept the terms that do not depend on x, and hence are the same in both the high- and low-temperature phases, separate. It is clear from these expressions that demanding $\mathrm{Re}\, f_{\mathrm{L}} = \mathrm{Re}\, f_{\mathrm{H}}$ gives us back exactly the same expression for the Fisher locus as in the random graph case, namely

$$|2(1 - c)^3| = |(1 + c)^2(1 - 2c)|. \tag{30}$$

The first two terms in each of equations (29) have been spirited away into the similarity sign in $f \sim \log \tilde{S}$ in the random graph expressions, where they arise from the normalizing $\det K$ in equation (10).

That the Bethe lattice with three neighbours should have the same Fisher zeros as the ϕ^3 random graph is not unexpected, since the ratio of the saddle point solutions for the random graph model gives precisely the recursion relation (26) and both exhibit mean-field critical behaviour. The fixed point of the recursion variable x in the Bethe lattice solution is equal to the ratio of the ϕ_+ and ϕ_- solutions in the random graph case. This equivalence between the random graph and Bethe lattice models is quite generic and also applies to the Potts models which we now move on to discuss.

5. Potts model on thin random graphs

A similar expression to equation (10) can be used to define the partition function for a q-state Potts model where the Hamiltonian can be written

$$-\beta H = \beta \sum_{\langle ij \rangle} (\delta_{\sigma_i, \sigma_j} - 1). \tag{31}$$

The spins σ_i now take on q values, so one might expect by analogy with the Ising model ($q = 2$) that q 'fields' ϕ might be needed. This leads to a Potts action of the form [17]

$$S = \tfrac{1}{2}\sum_{i=1}^{q} \phi_i^2 - c\sum_{i<j} \phi_i \phi_j - \tfrac{1}{3}\sum_{i=1}^{q} \phi_i^3 \tag{32}$$

with $c = 1/(\exp(2\beta) + q - 2)$. The description in terms of q ϕ_i fields turns out to be redundant at least as far as the saddle-point solution goes, since explicit solution for various q reveals that the ϕ_i only take on two values in the dominant low-temperature solutions and all are equal at high temperature[10]. It is thus possible to write down an effective saddle-point action in terms of just two fields $\phi = \phi_{1...q-1}$ and $\tilde{\phi} = \phi_q$

$$S_{\mathrm{L}} = \tfrac{1}{2}(q - 1)\left[1 - c(q - 2)\right]\phi^2 - \tfrac{1}{3}(q - 1)\phi^3 + \tfrac{1}{2}\tilde{\phi}^2 - \tfrac{1}{3}\tilde{\phi}^3 - c(q - 1)\phi\tilde{\phi}. \tag{33}$$

If we solve for $\phi, \tilde{\phi}$ we find the low-temperature solutions

$$\phi = \tfrac{1}{2} - \tfrac{1}{2}(q - 3)c - \tfrac{1}{2}\sqrt{(1 - 2cq + 2c + c^2q^2 - 6c^2q + 5c^2)}$$
$$\tilde{\phi} = \tfrac{1}{2} + \tfrac{1}{2}(q - 1)c + \tfrac{1}{2}\sqrt{(1 - 2cq + 2c + c^2q^2 - 6c^2q + 5c^2)} \tag{34}$$

as well as a high-temperature solution with $\phi = \tilde{\phi} = \phi_0$,

$$\phi_0 = 1 - (q - 1)c \tag{35}$$

---

[10] This is rather similar to the one-dimensional Potts model where due to the permutation symmetry (for $q \geqslant 2$) only two of the q eigenvalues in the transfer matrix contribute in the thermodynamic limit.
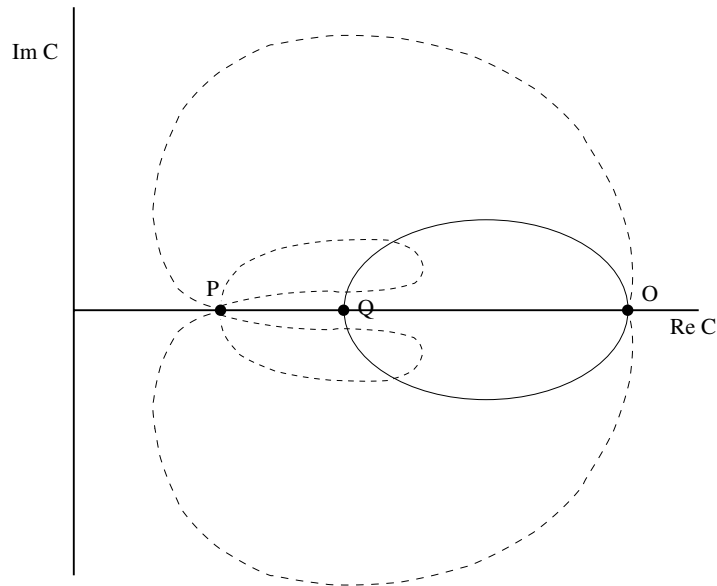
Figure 2. A schematic representation of the locus of Fisher zeros for a $q > 2$ state Potts model, in the complex $c = 1/(\exp(2\beta) + q - 2)$ plane. The dashed locus represents the metastable branch and would *not* give rise to partition function zeros, whereas the inner loop, drawn in bold, represents the true partition function zeros. The labelled points are the spinodal point $P = 1/(2q - 1)$, the 'true' first-order point $Q = (1 - (q - 1)^{-1/3})/(q - 2)$ and the point O at which the loci meet (which is outside the physical region $0 < c < 1/(q - 1)$).

and another branch of the solution reversing the signs in front of both square roots. These lead to a high-temperature saddle-point action

$$S_H = \frac{q}{6}(1 - (q - 1)c)^3 \tag{36}$$

and two unwieldy expressions for the saddle-point action S_L in the low-temperature regime, one coming from each branch of the ϕ solutions,

$$
\begin{aligned}
S_L = {}&-\tfrac{11}{6}c^3 + \tfrac{1}{12}q - \tfrac{1}{4}cq^2 - \tfrac{1}{12}c^3q^4 - \tfrac{3}{2}c^2q^2 - \tfrac{13}{4}c^3q^2 \\
&+ \tfrac{1}{4}c^2q^3 + \tfrac{9}{4}c^2q + \tfrac{11}{12}c^3q^3 - c^2 + \tfrac{17}{4}c^3q + \tfrac{3}{4}cq - \tfrac{1}{2}c \\
&\pm \tfrac{1}{12}(q - 2)(1 - 2cq + 2c + c^2q^2 - 6c^2q + 5c^2)^{3/2}.
\end{aligned}
\tag{37}
$$

The expressions for S_L become a lot more palatable when a particular q value is inserted. Just as for the Ising model the locus of Fisher zeros can now be obtained by demanding $|S_H| = |S_L|$ for complex c.

A schematic graph of the locus of zeros for general $q > 2$ is shown in figure 2, where it can be seen that the physical locus of zeros, shown in bold, crosses the real axis in the physical region of the parameter ($0 < c < 1/(q - 1)$) at the first-order transition point $Q = (1 - (q - 1)^{-1/3})/(q - 2)$. This physical locus lies inside a larger metastable locus, shown dashed, which has a cusp at the spinodal point $P = 1/(2q - 1)$. The loop in the Ising locus, which was excised by comparing the actions along the real axis, has split into the two dashed mirror inner loops lying off the axis in the Potts models. Referring back to figure 1 we can see that in the Ising case the first-order locus vanishes but the cusp remains and takes over the role of the physical locus. At Q we would assign $\alpha = 1$ for a first-order transition point
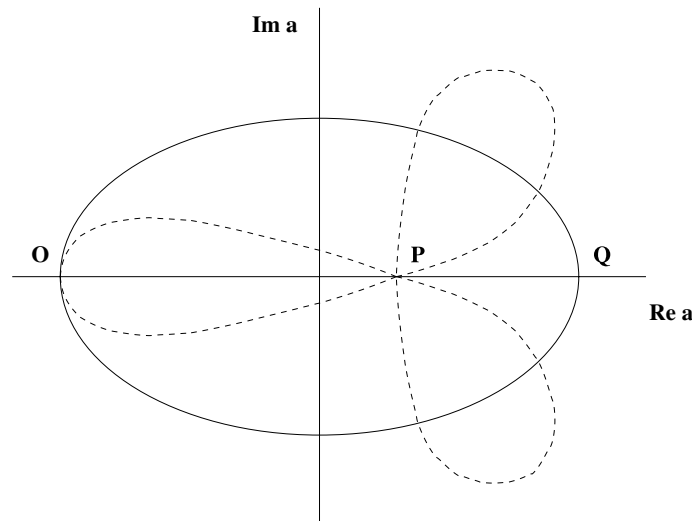
Figure 3. The locus of Fisher zeros for a $q > 2$ state Potts model, now in the complex $a = \exp(-2\beta)$ plane. The labelling is as in figure 2.

so the angle of approach to the real axis should be $\pi/2$ from equation (18), which is what is observed. The other crossing point O lies outside the physical region $0 < c < 1/(q-1)$.

Perhaps a slightly fairer comparison with the Ising model is to plot the loci in the $a = \exp(-2\beta)$ plane, which we have also done in figure 3. The outer ovoid is now the genuine locus of zeros and the metastable locus maps onto the tri-foliate structure that lies largely inside this. In the variable a the physical region is $0 \leqslant a \leqslant 1$.

6. Potts model and thin chromatic zeros

One particularly interesting feature of the Potts saddle-point solution is that q appears as a parameter, so it is possible to obtain the Fisher locus for non-integer or even complex q-values. This means that in principle one can also investigate the complex q-properties of the chromatic polynomials on the random graphs. The chromatic polynomial $P(G, q)$ on a given graph G of order n encodes the number of ways that G may be q-coloured so that no two adjacent vertices have the same colour. It is related to the partition function of the anti-ferromagnetic Potts model $Z(G, q, \beta = -\infty)$ on G in the zero-temperature limit,

$$Z(G, q, \beta = -\infty) = P(G, q). \tag{38}$$

We can follow Shrock and Tsai [18] and consider a limiting function $W(\{G\}, q)$ on some class of graphs $\{G\}$, in our case random regular graphs,

$$W(\{G\}, q) = \lim_{n \to \infty} P(G, q)^{1/n} \tag{39}$$

which is related to the free energy (per site) of the corresponding Potts model

$$f(G, q, \beta = -\infty) = \log W(\{G\}, q) \tag{40}$$

and gives us that the saddle-point action is effectively the limiting function, $\tilde{S}(G, q, \beta = -\infty) \sim W(\{G\}, q)$. Since $\beta \to -\infty$ corresponds to $c \to 1/(q-2)$ we can write down an action in this limit by making a suitable substitution for c in equation (33)

$$S = -\frac{1}{3}(q-1)\phi^3 + \frac{1}{2}\tilde{\phi}^2 - \frac{1}{3}\tilde{\phi}^3 - \frac{q-1}{q-2}\phi\tilde{\phi}. \tag{41}$$
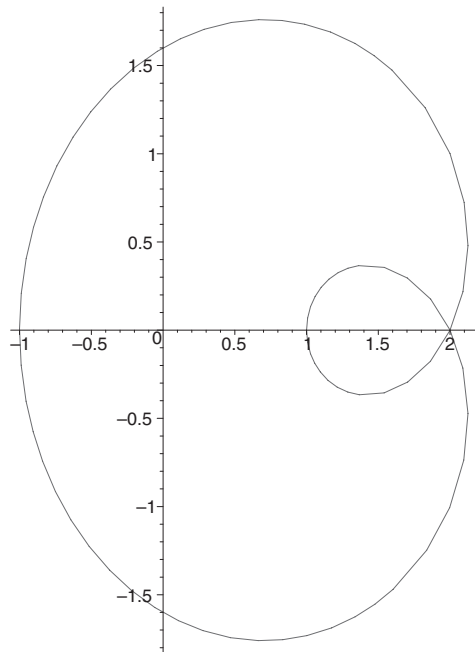
Figure 4. The locus of chromatic zeros for ϕ^3 graphs in the complex q-plane. The locus is given by the limaçon $((x-1)^2 + y^2 - 1)^2 - (x-2)^2 - y^2 = 0$ where $x = \mathrm{Re}\, q$ and $y = \mathrm{Im}\, q$.

Instead of looking for high- and low-temperature saddle-point solutions of this action, we are now interested in finding the 'high-q' (S_{H}, $\phi = \tilde{\phi}$) and 'low-q' (S_{L}, $\phi \neq \tilde{\phi}$) solutions, which are given by

$$\phi_0 = \phi = \tilde{\phi} = \frac{1}{2-q}$$

$$\phi = \frac{-1 \pm \sqrt{5-4q}}{2(2-q)} \tag{42}$$

$$\tilde{\phi}_\pm = \frac{(2q-3) \pm \sqrt{5-4q}}{2(q-2)}$$

respectively. We can now ape the procedure for finding the locus of Fisher zeros to determine the locus of chromatic zeros by examining the curves defined by $|S_{\mathrm{L}}| = |S_{\mathrm{H}}|$ in the complex q-plane rather than the complex c-plane. Although presented in a disguised form this turns out to be the limaçon of Pascal shown in figure 4, adding nicely to our collection of classical plane curves. We can see that, interestingly, the locus crosses the negative real axis, which is an unusual occurrence and merits closer investigation. None of the families of graphs considered in [18] displayed this property.

7. Discussion

We have seen that both Fisher and chromatic zero loci may be traced out on thin random graphs by adapting the approach of [10], which was originally formulated in the context of first-order phase transitions. We argued that even transitions that were continuous at the physical critical point would generically display first-order properties at all but a finite set of points and that

the formulae of equation (2) could thus still be employed. These gave a cusplike locus, similar to an amputated folium of Descartes, for the Ising Fisher zeros and a rather more complicated structure for the $q > 2$ Potts models, where the Ising-like cusp was still present as a metastable locus. The limiting chromatic zero locus on ϕ^3 graphs, remarkably, emerged as a limaçon. The Ising model on the Bethe lattice with three neighbours per site returned the same Fisher zeros as the ϕ^3 graphs by a rather different route, showing again the effective equivalence of the models.

We have not discussed the case of *planar* random graphs here, but a similar approach can be applied to the solutions of [15], and compared with the series expansions and Monte Carlo simulations of [8]. Similarly, we have concentrated entirely on Fisher zeros, but it is clear following [10] that one can also examine the behaviour of the Lee–Yang zeros.

In summary, noting that the locus of partition function zeros can be thought of as phase boundaries in the complex temperature plane gives a useful way of determining the locus of Fisher zeros in the thermodynamic limit for Ising and Potts models on random graphs, as well as chromatic zeros.

Acknowledgments

References

[1] Yang C N and Lee T D 1952 *Phys. Rev.* **87** 404
    Lee T D and Yang C N 1952 *Phys. Rev.* **87** 410
[2] Lebowitz J and Penrose O 1968 *Commun. Math. Phys.* **11** 99
    Baker G 1968 *Phys. Rev. Lett.* **20** 990
    Abe R 1967 *Prog. Theor. Phys.* **37** 1070
    Abe R 1967 *Prog. Theor. Phys.* **38** 72
    Abe R 1967 *Prog. Theor. Phys.* **38** 568
    Ono S, Karaki Y, Suzuki M and Kawabata C 1968 *J. Phys. Soc. Japan* **25** 54
    Gaunt D and Baker G 1970 *Phys. Rev.* B **1** 1184
    Kortman P and Griffiths R 1971 *Phys. Rev. Lett.* **27** 1439
    Fisher M 1978 *Phys. Rev. Lett.* **40** 1611
    Kurtze D and Fisher M 1979 *Phys. Rev.* B **20** 2785
    Fisher M 1965 *Lectures in Theoretical Physics* vol 7 C (Boulder, CO: University of Colorado Press)
[3] Itzykson C, Pearson R and Zuber J 1983 *Nucl. Phys.* B **220 [FS8]** 415
[4] Dammer S M, Dahmen S R and Hinrichsen H 2001 Directed percolation and the golden ratio *Preprint* cond-mat/0106396
    Arndt P F 2000 *Phys. Rev. Lett.* **84** 814
[5] Marchesini G and Schrock R 1989 *Nucl. Phys.* B **318** 541
    Matveev V and Shrock R 1995 *J. Phys. A: Math. Gen.* **28** 1557
    Matveev V and Shrock R 1996 *J. Phys. A: Math. Gen.* **29** 803
    Matveev V and Shrock R 1995 *J. Phys. A: Math. Gen.* **28** 4859
    Matveev V and Shrock R 1995 *J. Phys. A: Math. Gen.* **28** 5235
    Matveev V and Shrock R 1995 *J. Phys. A: Math. Gen.* **28** L533–9
    Matveev V and Shrock R 1995 *Phys. Lett.* A **204** 353
    Matveev V and Shrock R 1996 *Phys. Rev.* E **53** 254

Matveev V and Shrock R 1996 *Phys. Lett.* A **215** 271
Matveev V and Shrock R 1996 *Phys. Rev.* E **54** 6174
[6] Kim S-Y and Creswick R J 1998 *Phys. Rev.* E **58** 7006
Kim S-Y and Creswick R J 1998 *Phys. Rev. Lett.* **81** 2000
Kim S-Y and Creswick R J 2000 *Physica* A **281** 252
Kim S-Y and Creswick R J 2000 *Physica* A **281** 262
[7] Repetowicz P, Grimm U and Schreiber M 2000 *Mater. Sci. Eng.* A **294–6** 638
[8] Ambjorn J, Anagnostopoulos K and Magnea U 1997 *Mod. Phys. Lett.* A **12** 1605
Ambjorn J, Anagnostopoulos K and Magnea U 1998 *Nucl. Phys. (Proc. Suppl.)* **63** 751
[9] de Albuquerque L C, Alves N A and Dalmazi D 2000 *Nucl. Phys.* B **580** 739
[10] Biskup M, Borgs C, Chayes J T, Kleinwaks L J and Kotecky R 2000 *Phys. Rev. Lett.* **84** 4794
Biskup M, Borgs C, Chayes J T, Kleinwaks L J and Kotecky R 2001 Partition function zeros at first-order phase transitions *Preprint*
[11] Monroe J L 1996 *J. Phys. A: Math. Gen.* **29** 5421
Monroe J L 1991 *J. Stat. Phys.* **65** 255
Wagner F, Grensing D and Heide J 2000 *J. Phys. A: Math. Gen.* **33** 929
Akheyan A Z, Ananikian N S and Dallakian S K 1998 *Phys. Lett.* A **242** 111
Ananikian N S, Dallakian S K, Izmailian N Sh and Oganessyan K A 1996 *Phys. Lett.* A **214** 205
Ananikian N S, Dallakian S K, Izmailian N Sh and Oganessyan K A 1996 *Phys. Lett.* A **221** 434 (erratum)
Ananikian N S, Dallakian S K, Izmailian N Sh and Oganessyan K A 1997 *Fractals* **5** 175
Ananikian N S and Dallakian S K 1997 *Physica* D **107** 75
Ananikian N S, Dallakian S.K, Izmailian N Sh, Oganessyan K A and Hu B 1998 *Phys. Lett.* A **248** 381
Dolan B P 1995 *Phys. Rev.* E **52** 4512–5
Dolan B P 1996 *Phys. Rev.* E **53** 6590 (erratum)
[12] Bachas C, de Calan C and Petropoulos P M S 1994 *J. Phys. A: Math. Gen.* **27** 6121
[13] Baillie C F, Johnston D A and Kownacki J-P 1994 *Nucl. Phys.* B **432** 551
Baillie C F, Janke W, Johnston D A and Plechac P 1995 *Nucl. Phys.* B **450** 730
[14] Glumac Z and Uzelac K 1994 *J. Phys. A: Math. Gen.* **27** 7709
Dolan B and Johnston D 2000 1D Potts, Yang–Lee edges and chaos *Preprint* cond-mat/0010372
[15] Kazakov V A 1986 *Phys. Lett.* A **119** 140
[16] Baxter R 1982 *Exactly Soluble Models in Statistical Mechanics* (London: Academic)
Boulatov D V and Kazakov V A 1987 *Phys. Lett.* B **186** 379
Burda Z and Jurkiewicz J 1989 *Acta Phys. Polon.* B **20** 949
[17] Johnston D A and Plechac P 1997 *J. Phys. A: Math. Gen.* **30** 7349
[18] Shrock R and Tsai S-H 1997 *Phys. Rev.* E **55** 5165
Shrock R and Tsai S-H 1997 *Phys. Rev.* E **56** 1342
Shrock R and Tsai S-H 1997 *Phys. Rev.* E **56** 3935
Shrock R and Tsai S-H 1997 *Phys. Rev.* E **55** 6791–4
Shrock R and Tsai S-H 1997 *Phys. Rev.* E **56** 2733–7
Shrock R and Tsai S-H 1997 *Phys. Rev.* E **56** 4111–24
Shrock R and Tsai S-H 1998 *Physica* A **259** 315
Shrock R and Tsai S-H 1999 *J. Phys. A: Math. Gen.* **32** L195
Shrock R and Tsai S-H 1999 *J. Phys. A: Math. Gen.* **32** 5053
Shrock R and Tsai S-H 2000 *Physica* A **275** 429–49
Roček M, Shrock R and Tsai S-H *Physica* A **252** 505
Roček M, Shrock R and Tsai S-H *Physica* A **259** 367
Biggs N L and Shrock R 1999 *J. Phys. A: Math. Gen.* **32** L489
Chang S-C and Shrock R 2000 *Physica* A **286** 189–238
Chang S-C and Shrock R 2001 *Physica* A **290** 402
Chang S-C and Shrock R 2001 *Physica* A **292** 307
Chang S-C and Shrock R 2001 *Physica* A **296** 131
Chang S-C and Shrock R 2001 *Physica* A **296** 183
Chang S-C and Shrock R 2001 *Physica* A **296** 234